

Robust angle-based transfer learning in high dimensions

Tian Gu¹, Yi Han^{1,2}, and Rui Duan^{1,†}

¹Department of Biostatistics, Harvard T.H. Chan School of Public Health,
Boston, MA 02115, USA

² School of Mathematical Sciences, Shanghai Jiaotong University,
Shanghai, 200240, China

† Corresponding author: rduan@hsph.harvard.edu

Abstract

Transfer learning aims to improve the performance of a target model by leveraging data from related source populations. It is known to be especially helpful in cases with insufficient target data. In this paper, we study the problem of how to train a high-dimensional ridge regression model with limited target data and existing models trained in heterogeneous source populations. We consider a practical setting where only the source model parameters are accessible, instead of the individual-level source data. Under the setting with only one source model, we propose a novel flexible angle-based transfer learning (angleTL) method, which leverages the concordance between the source and the target model parameters. We show that angleTL unifies several benchmark methods by construction, including the target-only model trained using target data alone, the source model trained using the source data, and the distance-based transfer learning method that incorporates the source model to the target training by penalizing the difference between the target and source model parameters measured by the L_2 norm. We also provide algorithms to effectively incorporate multiple source models accounting for the fact that some source models may be more helpful than others. Our high-dimensional asymptotic analysis provides interpretations and insights regarding when a source model can be helpful to the target model, and demonstrates the superiority of angleTL over other benchmark methods. We perform extensive simulation studies to validate our theoretical conclusions and show the feasibility of applying angleTL to transfer existing genetic risk prediction models across multiple biobanks.

1 Introduction

Training a model with insufficient data is a common problem in practice. For example, limited user credit history data is available for individual financial risk evaluation and fraud detection (Teja, 2017). In precision medicine research, limited data from medical records are available to study rare conditions (Jia and Shi, 2017) or underrepresented minority and disadvantaged sub-populations, which has restricted the fairness and clinical impact (Kim and Milliken, 2019) of precision medicine. In situations with limited training data, researchers seek to leverage available external data sources to boost model performance (Viele et al., 2014; Li and Song, 2020; Yang and Kim, 2020).

When borrowing information from external sources, a major challenge is to account for the potential data heterogeneity. The external data may likely be collected from a different population with diverse characteristics (Chen et al., 2020) or be historical data where the variable definitions and measures may change over time (Mansukhani et al., 2019; Mitchell et al., 2021). Many data integration methods are proposed to address data heterogeneity while leveraging potentially shared information across populations. For example, some methods are based on re-weighting or re-sampling the source data such that they are more similar to the target (Huang et al., 2006; Pan et al., 2010; Long et al., 2013); some methods assume there is a unique lower dimensional representation of features across populations, which can be transferred from the source to the target (Tzeng et al., 2014; Ganin and Lempitsky, 2015; Sun and Saenko, 2016); some methods propose to use the target data to calibrate the source models (Girshick et al., 2014; Li et al., 2020; Gu et al., 2023). The performance of many of the above methods largely depends on whether the underlying assumptions regarding the similarity between the source and the target populations hold, which is usually unknown in practice. Therefore, it is desired to have methods that can adapt to the underlying data heterogeneity or at least prevent the case where incorporating the source information leads to worse model performance than not including it, known as the “negative transfer” phenomenon Weiss et al. (2016).

Another challenge is the data sharing constraints in the sense that external sources often cannot share individual-level data with the target study. Federated or distributed algorithms are proposed to overcome such data-sharing barriers by sharing only summary-level statistics across studies, many of which rely on sharing the gradients or higher-order derivatives of objective functions (Duan et al., 2018, 2020, 2022; Cai et al., 2021; Li et al., 2021) and may require iteratively communicating summary statistics across datasets (Cai et al., 2021; Li et al., 2021). However, distributed or federated learning is less feasible without a collaborative environment or infrastructure that enables calculating the required intermediate results and timely information sharing. In contrast, model parameters from existing studies are often more accessible. With increasing attention to reproducibility and open science, more journals require studies to publish all study results as supplementary materials or make them shareable upon request (Thompson et al., 2006; Roobol et al., 2012). Many platforms allow direct implementation (Belbasis and Panagiotou, 2022) or validation of fitted models on secure collaborative platforms such as PheKB (Kirby et al., 2016) and FATE (Liu et al., 2021).

There is an increasing need for data integration methods that can directly leverage fitted models to improve a target study.

In this paper, we consider the problem of how to incorporate fitted regression models from external sources to improve the model estimation and prediction accuracy in a target population with limited data. Regression models are broadly applied in many fields, due to advantages such as simplicity, computational efficiency, and interpretability (Hafemeister and Satija, 2019; Wynants et al., 2020; Wu et al., 2020), and they are also the building blocks of many data analysis pipelines and tools (Van Buuren et al., 2006; Tan, 2006). For the i -th subject in the target data, let $\mathbf{Y}_i \in \mathbb{R}$ denote the outcome variable of interest and $\mathbf{X}_i \in \mathbb{R}^p$ denote a set of p -dimensional covariates. We assume that

$$\mathbf{Y}_i = \mathbf{X}_i^\top \boldsymbol{\beta} + \epsilon_i, \quad \text{for } i \in \{1, \dots, n\}$$

where $\epsilon_i \in \mathbb{R}$ is the random noise with mean zero and variance σ^2 , $\boldsymbol{\beta} \in \mathbb{R}^p$ is the regression coefficient to be estimated, and n is the target sample size. In addition to the target data, we observe a source model fitted on an external source dataset, where we have the parameter estimate $\hat{\mathbf{w}} \in \mathbb{R}^p$ for the underlying regression coefficient \mathbf{w} in the source population. In the case where the underlying coefficients, $\boldsymbol{\beta}$ and \mathbf{w} , share certain similarities, we hope to leverage $\hat{\mathbf{w}}$ to assist the estimation of the target parameter, $\boldsymbol{\beta}$.

Similar problems have been considered in some related work. In a series of transfer learning work, the source model estimates $\hat{\mathbf{w}}$ was incorporated as a regularization with the form $\|\boldsymbol{\beta} - \hat{\mathbf{w}}\|_q$, for some positive constant q . For example, Li et al. (2020) proposed the TransLASSO algorithm that leveraged the source data by penalizing $\|\boldsymbol{\beta} - \hat{\mathbf{w}}\|_1$ when learning $\boldsymbol{\beta}$ using the target data. Later, TransLASSO has been extended to generalized linear models (Tian and Yang, 2022), functional linear regression (Lin and Reimherr, 2022), and Q-learning (Chen et al., 2022). Considering data sharing constraints, Li et al. (2021) proposed a federated learning approach by sharing gradients and Hessian matrices, and Gu et al. (2022) proposed a method to incorporate information from fitted models through a synthetic data approach. Similar ideas are also seen in multi-tasking learning literature, where $L2$ -norm-based constraints or penalties, i.e., $\|\boldsymbol{\beta} - \mathbf{w}\|_2$, are introduced to leverage the similarities between model parameters (Tian et al., 2022; Duan and Wang, 2022). Since the common underlying assumption of the above methods is that the distance of the two underlying true parameters, i.e., $\|\boldsymbol{\beta} - \mathbf{w}\|_q$, is small, we refer to this class of method as the distance-based transfer learning. According to the theoretical analyses in Li et al. (2020), the performance of the distance-based transfer learning depends on the magnitude of $\|\boldsymbol{\beta} - \mathbf{w}\|_q$.

In real-world applications, the distance-based transfer learning methods may be less effective when $\boldsymbol{\beta}$ and \mathbf{w} are highly concordant, but their distance may not be small. For example, the source outcome may be defined differently from the target outcome (categorical versus continuous), or there is some standardization procedure applied to the source data that is unknown to us, or the source model is fitted using a different but related outcome that is highly correlated with the target outcome (Miglioretti, 2003; Stearns, 2010). In addition, distributional shift of the covariate

variables may also cause the underlying \mathbf{w} to be different from β under model mis-specification. Several alternative characterizations of model similarity are proposed. For example, Li et al. (2014) proposed a bivariate ridge regression, assuming $(\beta_j, \mathbf{w}_j)^\top$ follow a bivariate normal distribution with correlation ρ . Similarly, Maier et al. (2014) proposed a multi-traits prediction method, assuming multivariate normally distributed random effects to leverage shared genetic architectures across traits. Liang et al. (2020) proposed a calibration version of TransLASSO, which allows the scale of the model parameters to differ. However, these methods require individual-level data and their robustness is unclear when data heterogeneity is high.

In this paper, we propose an **angle**-based **T**ransfer **L**earning approach, named angleTL, that quantifies the similarity of two regression models through the angle between the regression coefficients. We build angleTL on a high-dimensional ridge regression model (Hoerl and Kennard, 1970), which enjoys computational simplicity and does not require restricted sparsity conditions on model parameters. In the case of a single source model, we show that angleTL unifies several benchmark methods by construction, including the target-only model trained using target data alone, the source model trained using the source data, and the distance-based transfer learning method that incorporates the source model to the target training by penalizing the difference between the target and source model parameters measured by the L_2 norm. With multiple source models, we propose methods to effectively incorporate them toward better predictive performance in the target population. The proposed methods only require fitted source models, which are more accessible in practice. We provide high-dimensional asymptotic analyses that precisely quantify the predictive error of angleTL. Our theoretical analyses provide interpretations and insights regarding when a source model can be helpful to the target, and demonstrate the superiority of angleTL over other benchmark methods. We perform extensive simulation studies to validate our theoretical conclusions and evaluate the performance of angleTL by training genetic risk models for low-density lipoprotein cholesterol (LDL) using data from multiple large-scale biobanks.

2 Angle-based Transfer Learning Method

Let $\mathbf{Y} \in \mathbb{R}^n$ denote the outcome variable of interest and $\mathbf{X} \in \mathbb{R}^{n \times p}$ denote a set of p -dimensional covariates in the target data of size n . Without borrowing information from the source, we can obtain a *target-only estimator* of β through a ridge regression, i.e.,

$$\tilde{\beta}_\lambda = \arg \min_{\beta} \frac{1}{n} \|\mathbf{Y} - \mathbf{X}\beta\|_2^2 + \lambda \|\beta\|_2^2, \quad (1)$$

where λ is a tuning parameter.

Suppose that we also observe $\hat{\mathbf{w}} \in \mathbb{R}^p$, the parameter estimates of a source model fitted on an external source dataset with a sample size potentially much larger than the target data. Due to data heterogeneity, the two underlying regression coefficients, β and \mathbf{w} , may not be the same but may share certain similarities, and hence $\hat{\mathbf{w}}$ can be used to guide the estimation of β . Following a series of recent transfer learning methods (Li et al., 2022, 2021; Gu et al., 2022), we define the

distance-based transfer learning estimator (distTL) to be

$$\hat{\beta}_{\lambda_d} = \arg \min_{\beta} \frac{1}{n} \|\mathbf{Y} - \mathbf{X}\beta\|_2^2 + \lambda_d \|\beta - \hat{\mathbf{w}}\|_2^2, \quad (2)$$

where λ_d is a tuning parameter. Imposing a distance-based penalty, $\|\beta - \hat{\mathbf{w}}\|_2$, is equivalent to adding a constraint $\|\beta - \hat{\mathbf{w}}\|_2 \leq h$, which reduces the parameter space to a L_2 ball centered at $\hat{\mathbf{w}}$ as shown in the left panel of Figure 1. Anchoring on the source estimator $\hat{\mathbf{w}}$, distTL encourages estimators closer to $\hat{\mathbf{w}}$ while allowing for the calibration of potential differences.

As introduced earlier, in real-world applications, it is possible that β and \mathbf{w} are concordant to some degree, but $\|\beta - \mathbf{w}\|_2$ is not small. In such cases, distTL may be less effective for leveraging the existing source model. Therefore, we propose a more general characterization of the similarity using the $\sin \Theta$ distance between \mathbf{w} and β . As shown in the right panel of Figure 1, if the target model parameter β is restricted by a constraint that $\sin \Theta(\beta, \mathbf{w}) \leq d$, the source model \mathbf{w} can provide information on the direction of β and reduce the parameter space of β to a cone. When \mathbf{w} and β are small in L_2 distance, it also implies that the angle between the two vectors is small, while it may not be true in the opposite way.

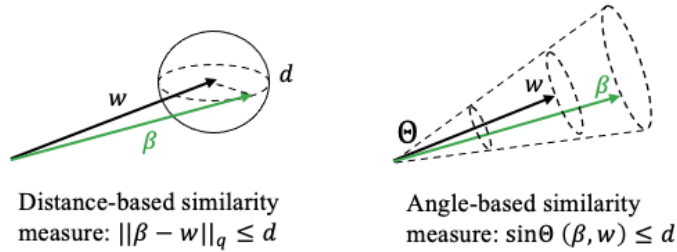


Figure 1: Geometric illustration of the distance-based similarity characterization (left) and the proposed angle-based characterization (right).

Unlike distTL that directly translates the similarity assumption into a penalty term in the optimization, penalizing on $\sin \Theta(\hat{\mathbf{w}}, \beta) = \sqrt{1 - \frac{(\hat{\mathbf{w}}^\top \beta)^2}{\|\hat{\mathbf{w}}\|_2^2 \|\beta\|_2^2}}$ leads to computational difficulty due to its non-convex form. We propose the following easy-to-implement *angle-based transfer learning estimator* defined as

$$\hat{\beta}_{\lambda, \eta} = \arg \min_{\beta} \frac{1}{n} \|\mathbf{Y} - \mathbf{X}\beta\|_2^2 + \lambda \|\beta\|_2^2 - 2\eta \hat{\mathbf{w}}^\top \beta, \quad (3)$$

where λ and η are tuning parameters. The proposed optimization problem in Equation (3) is equivalent to adding an extra penalty term $-2\hat{\mathbf{w}}^\top \beta$ to the standard target-only ridge regression in Equation (1). Intuitively, with fixed $\hat{\mathbf{w}}$ and $\|\beta\|_2$, the extra penalty is small if $\hat{\mathbf{w}}$ and β are more concordant while it is large when their directions are diverse.

The proposed optimization problem has several advantages. First, given λ and η , the optimization has a closed-form solution $\hat{\beta}_{\lambda,\eta} = (\mathbf{X}^\top \mathbf{X} + n\lambda \mathbf{I}_n)^{-1}(\mathbf{X}^\top \mathbf{Y} + n\eta \hat{\mathbf{w}})$, which improves computational efficiency. More importantly, it incorporates several estimators as special cases: (i) when $\eta = 0$, $\hat{\beta}_{\lambda,\eta}$ reduces to the target-only estimator shown in Equation (1), (ii) when $\eta = \lambda$, $\hat{\beta}_{\lambda,\eta}$ becomes distTL in Equation (2), since the optimization remains the same if we add an additional β -independent term $\lambda \|\hat{\mathbf{w}}\|_2^2$, i.e., $\lambda \|\beta\|_2^2 - 2\lambda \hat{\mathbf{w}}^\top \beta + \lambda \|\hat{\mathbf{w}}\|_2^2 = \lambda \|\beta - \hat{\mathbf{w}}\|_2^2$; and (iii) if η is extremely large, the penalty term $-2\eta \hat{\mathbf{w}}^\top \beta$ will dominate and result in $\beta \approx c\hat{\mathbf{w}}$, the same as rescaling the source estimator by a constant c .

Using cross-validation, we can select the optimal λ and η from a grid covering a proper range. As one of the main advantages of the proposed method, in light of the above discussions, we expect that under suitable conditions, the numerical performance of angleTL will be no worse than the target-only, source-rescaling, or distTL. In particular, the guaranteed performance with respect to the target-only method implies that our method automatically prevents negative transfer without needing a validation dataset, which has great benefits in practice. In Section 3, we will elaborate on these points under a rigorous theoretical framework, and provide precise characterizations of angleTL’s performance, revealing its scope of applicability and the advantages over alternative approaches.

3 Predictive Risk and Theoretical Justifications

In this section, we study the predictive risk of $\hat{\beta}_{\lambda,\eta}$ in Equation (3). For a given choice of λ and η , we denote the prediction risk by

$$r_{\lambda,\eta}(\mathbf{x}) = \mathbb{E}\{(\mathbf{x}^\top \hat{\beta}_{\lambda,\eta} - \mathbf{y})^2 | \mathbf{X}\}$$

where \mathbf{X} is the training data, and the expectation is taken over an independent test data point (\mathbf{x}, \mathbf{y}) , from the same distribution as the training data. Given λ and η , we denote $\mathcal{R}(\lambda, \eta) = \lim_{(n,p) \rightarrow \infty} r_{\lambda,\eta}(\mathbf{X})$, the limiting prediction risk as the training sample size n and the dimension p go to infinity. Our theoretical analysis is based on the following assumptions.

Assumption 1. (High-Dimensional Asymptotics) *The following conditions hold:*

- (a) *The dimension of the model, p , goes to infinity as n goes to infinity, with $\frac{p}{n} \rightarrow \gamma \in (0, \infty)$.*
- (b) *The target data, $\mathbf{X} \in \mathbb{R}^{n \times p}$, consists of identically and independently rows with mean zero and covariance matrix Σ , which is positive semidefinite.*
- (c) *The cumulative distribution function of the eigenvalues, i.e., the spectral distribution, F_Σ of Σ converges to a limit population spectral distribution on the support $[0, \infty)$.*

Assumption 2. (Random Regression Coefficients) *The target regression coefficients, $\beta \in \mathbb{R}^p$, are random with $\mathbb{E}[\beta] = \mathbf{0}$, and $\text{Var}[\beta] = \frac{\alpha_t^2}{p} \mathbf{I}_p$. The source coefficient \mathbf{w} are random with $\mathbb{E}[\mathbf{w}] = \mathbf{0}$ and $\text{Var}[\mathbf{w}] = \frac{\alpha_s^2}{p} \mathbf{I}_p$. The coefficients β and \mathbf{w} satisfy $\text{Cov}(\beta, \mathbf{w}) = \frac{\rho \alpha_t \alpha_s}{p} \mathbf{I}_p$.*

Assumption 3. (Source Estimation Error) The obtained source estimator $\hat{\mathbf{w}}$ can be decomposed as $\hat{\mathbf{w}} = \mathbf{w} + \boldsymbol{\delta}$, where $\boldsymbol{\delta}$ is some sub-Gaussian estimation error vector independent of \mathbf{w} and $\boldsymbol{\beta}$, with $\mathbb{E}[\boldsymbol{\delta}\boldsymbol{\delta}^\top] = \frac{1}{p}\boldsymbol{\Sigma}_\delta$. We assume that as $(n, p) \rightarrow \infty$, the eigenvalues of $\boldsymbol{\Sigma}_\delta$ is supported on $[C_L, C_U]$ for some constants $C_U \geq C_L \geq 0$.

A few remarks on the above assumptions are in order. In general, these assumptions together help us leverage results from random matrix theory to precisely compute the prediction risk of the proposed method, and enable rigorous comparisons with alternative methods. In particular, Assumption 1(a) concerns the limit of the ratio $\frac{p}{n}$ as $n \rightarrow \infty$, reflecting the high-dimensional nature of the problem. Assumption 1(b) is a mild condition on the design matrix, which requires independent samples but allows general correlations among high-dimensional covariates. Assumption 1(c) ensures the existence of proper limit for the eigenvalues of the underlying covariance matrix $\boldsymbol{\Sigma}$ as $p \rightarrow \infty$, which can be satisfied by a large class of covariance matrices with diagonal, exchangeable, or auto-regressive structures. Assumption 2 characterizes the signal strength by considering random regression coefficients and imposing moment conditions for their distribution. Under Assumption 2, the signal strength in the target model is characterized by the quantity α_t^2 , which is scaled by $\frac{1}{p}$ so that $\mathbb{E}\|\boldsymbol{\beta}\|_2^2 = \alpha_t^2$ and $\mathbb{E}\|\mathbf{w}\|_2^2 = \alpha_s^2$. Finally, Assumption 3 characterizes the estimation error of the source estimate $\hat{\mathbf{w}}$ for estimating \mathbf{w} .

Before stating our main theorem, we define a complex function $v(z) : \mathbb{C} \setminus \mathbb{R}^+ \rightarrow \mathbb{C}$, which plays an important role in our description of the prediction risk $\mathcal{R}(\lambda, \eta)$. Specifically, according to Assumption 1, the spectral distribution of the $n \times n$ matrix $\frac{1}{n}\mathbf{X}\mathbf{X}^\top$ has a limit, which we denote as $F_{\underline{\boldsymbol{\Sigma}}}$. In particular, $F_{\underline{\boldsymbol{\Sigma}}}$ is related to $F_{\boldsymbol{\Sigma}}$ in Assumption 1(c) via the equation

$$F_{\underline{\boldsymbol{\Sigma}}}(x) - \gamma F_{\boldsymbol{\Sigma}}(x) = (1 - \gamma)1\{x = 0\}.$$

We define $v(z)$ to be the Stieltjes transform of the probability measure $F_{\underline{\boldsymbol{\Sigma}}}$, i.e.,

$$v(z) := \int_0^\infty \frac{dF_{\underline{\boldsymbol{\Sigma}}}(x)}{x - z}, \quad z \in \mathbb{C} \setminus \mathbb{R}^+.$$

Theorem 1. Under Assumptions 1-3, as $n \rightarrow \infty$, the limiting expected predictive risk $\mathcal{R}(\lambda, \eta)$ satisfies

$$R(\lambda, \eta, C_L) \leq \mathcal{R}(\lambda, \eta) \leq R(\lambda, \eta, C_U),$$

where

$$R(\lambda, \eta, C) := (\lambda^2\alpha_t^2 + \eta^2\alpha_s^2 + \eta^2C - 2\lambda\eta\rho\alpha_t\alpha_s) \frac{v(-\lambda) - \lambda v'(-\lambda)}{\gamma(\lambda v(-\lambda))^2} + \frac{\sigma^2 v'(-\lambda)}{v(-\lambda)}.$$

The minimal risk $\mathcal{R}^* = \min_{\lambda, \eta} \mathcal{R}(\lambda, \eta)$ under the optimal choice of tuning parameters satisfies

$$\frac{\sigma^2}{\lambda_L^* v(-\lambda_L^*)} \leq \mathcal{R}^* \leq \frac{\sigma^2}{\lambda_U^* v(-\lambda_U^*)},$$

where $\lambda_L^* = \frac{\gamma\sigma^2}{\alpha_t^2(1 - \frac{\rho^2\alpha_s^2}{\alpha_s^2 + C_L})}$ and $\lambda_U^* = \frac{\gamma\sigma^2}{\alpha_t^2(1 - \frac{\rho^2\alpha_s^2}{\alpha_s^2 + C_U})}$.

The proof of the above theorem can be found in the Supplementary Material, which relies on the asymptotic theory of eigenvalues of large random matrices and in particular the theoretical framework developed by (Dobriban and Wager, 2018) for the analysis of ridge-penalized linear regression and linear discrimination analysis. Similar techniques have been used for the precise analysis of many other high-dimensional problems such as covariance matrix estimation (Ledoit and Wolf, 2015; Cai et al., 2020, e.g.), low-rank matrix denoising (Donoho and Gavish, 2014, e.g.), sketching and random projection (Yang et al., 2021, e.g.), etc.

Theorem 1 provides upper and lower bounds for the limiting prediction risk $\mathcal{R}(\lambda, \eta)$ as a function of the parameters λ and η . The possible range of $\mathcal{R}(\lambda, \eta)$ is rooted in the variability of the source estimator $\hat{\mathbf{w}}$. More specifically, the upper and lower bounds for $\mathcal{R}(\lambda, \eta)$ are determined by the spectrum of Σ_δ in Assumption 3, which in general decreases as the estimation error δ becomes smaller. In addition, the difference between the upper and the lower bounds $R(\lambda, \eta, C_U) - R(\lambda, \eta, C_L) = \frac{(C_U - C_L)\eta^2[v(-\lambda) - \lambda v'(-\lambda)]}{\gamma(\lambda v(-\lambda))^2}$ depends on the spectral range $(C_U - C_L)$ of Σ_δ , which becomes smaller when the components of δ are less heteroskedastic or less correlated.

Moreover, the minimal risk \mathcal{R}^* lies in the interval $[\frac{\sigma^2}{\lambda_L^* v(-\lambda_L^*)}, \frac{\sigma^2}{\lambda_U^* v(-\lambda_U^*)}]$. To better understand its implications, we consider a few special scenarios of interest, and assume for simplicity that the population spectral distribution F_Σ is supported on a set bounded away from zero and infinity and $C_L = C_U = C$. In this case, our predictive risk is precise with $\mathcal{R}^* = \frac{\sigma^2}{\lambda^* v(-\lambda^*)}$ where $\lambda^* = \frac{\gamma \sigma^2}{\alpha_t^2 (1 - \frac{\rho^2 \alpha_s^2}{\alpha_s^2 + C})}$ and $\eta^* = \lambda^* \frac{\rho \alpha_t \alpha_s}{\alpha_s^2 + C}$. On the one hand, when the target signal strength is very large, i.e., $\alpha_t^2 \rightarrow \infty$, we have that

$$\mathcal{R}^* \rightarrow \frac{\sigma^2}{1 - \gamma}, \quad \text{when } \gamma < 1 \quad (4)$$

and

$$\mathcal{R}^* = \frac{\alpha_t^2 (1 - \frac{\rho^2 \alpha_s^2}{\alpha_s^2 + C})}{\gamma v(0)} (1 + o(1)), \quad \text{when } \gamma > 1. \quad (5)$$

In other words, when $\gamma < 1$ and $\alpha_t^2 \rightarrow \infty$, the prediction risk reduces to that of the ordinary least squares, and is independent of the covariance Σ and the source data (such as ρ , α_s^2 , or C). When $\gamma > 1$, the limiting error as $\alpha_t^2 \rightarrow \infty$ depends on the covariance Σ through $v(0)$, and the source estimator through $1 - \frac{\rho^2 \alpha_s^2}{\alpha_s^2 + C}$. In the special case where $\Sigma = \mathbf{I}_p$, we have $v(0) = \frac{1}{\gamma - 1}$, so that the prediction risk decreases when the sample size increases, when the source-target similarity ρ^2 increases, or when the relative source estimation error $\frac{C}{\alpha_s^2}$ decreases. On the other hand, when the target signal strength is very small, i.e., $\alpha_t^2 \rightarrow 0$, we have

$$\mathcal{R}^* = \sigma^2 + \alpha_t^2 (1 - \frac{\rho^2 \alpha_s^2}{\alpha_s^2 + C}) T (1 + o(1)), \quad (6)$$

where $T = \lim_{n \rightarrow \infty} \frac{1}{p} \text{tr}(\Sigma)$, so that the difficulty of the prediction is determined to the first order by the average variance of the covariates and the source data, which does not depend on γ .

Another scenario of interest is when the source data has strong signal-to-noise ratio or contains extremely large sample size such that the estimation error of source model is negligible, i.e.,

$\frac{\alpha_s^2}{\alpha_s^2 + C_U} \rightarrow 0$. In this case, the point-wise limiting predictive risk becomes

$$\mathcal{R}_0(\lambda, \eta) = R(\lambda, \eta, 0) = (\lambda^2 \alpha_t^2 + \eta^2 \alpha_s^2 - 2\lambda\eta\rho\alpha_t\alpha_s) \frac{v(-\lambda) - \lambda v'(-\lambda)}{\gamma(\lambda v(-\lambda))^2} + \sigma^2 \frac{v'(-\lambda)}{v(-\lambda)}. \quad (7)$$

Under the optimal choice of tuning parameters $\lambda^* = \frac{\gamma\sigma^2}{\alpha_t^2(1-\rho^2)}$ and $\eta^* = \lambda^* \rho \frac{\alpha_t}{\alpha_s}$, we obtain $\mathcal{R}_0^* = \frac{\sigma^2}{\lambda^* v(-\lambda^*)}$. The proofs of Equations (4) to (7) can be found in the Supplementary Material.

The significance of Theorem 1 also lies in its implications on the practical benefits of the proposed method. On the one hand, it suggests that angleTL can automatically avoid negative transfer due to imprecise or low-quality source estimators, with performance no worse than the target-only estimator. Specifically, the limiting predictive risk of the target-only estimator $\tilde{\beta}_\lambda$ has been obtained in Dobriban and Wager (2018), which has a minimum risk $\mathcal{R}^\dagger = \frac{\sigma^2}{\lambda^\dagger v(-\lambda^\dagger)}$ under the optimal choice of tuning parameters $\lambda^\dagger = \gamma \frac{\sigma^2}{\alpha_t^2}$. As a comparison, the minimal risk \mathcal{R}^* of the angleTL estimator is always smaller than \mathcal{R}^\dagger . To see this, we first notice that \mathcal{R}^* is bounded by $R_U^* = \frac{\sigma^2}{\lambda_U^* v(-\lambda_U^*)}$. Since $\frac{1}{\lambda v(-\lambda)}$ is monotonically decreasing with λ , $\lambda^\dagger = \gamma \frac{\sigma^2}{\alpha_t^2} \leq \lambda^* = \frac{\gamma\sigma^2}{\alpha_t^2(1-\frac{\rho^2\alpha_s^2}{\alpha_s^2+C_U})}$ for any $\rho \geq 0$, $\alpha_s^2 \geq 0$ and $C_U > 0$, we have that $\mathcal{R}^* \leq R_U^* \leq \mathcal{R}^\dagger$. This indicates that the angleTL estimator safeguards against negative transfer because angleTL is always no worse than the target-only estimator, even when source has a large distance to the target (i.e., ρ is small), or the estimation error is large (i.e., $\frac{\alpha_s^2}{\alpha_s^2 + C_U}$ is small). The same property is achieved in Li et al. (2020) and Li et al. (2021) using an independent validation dataset, which is not required in our method.

Furthermore, angleTL is expected to have better performance than distTL. Specifically, since distTL is obtained by setting $\lambda = \eta$, under the current framework, its predictive risk is higher than the predictive risk of angleTL, as \mathcal{R}^* is optimized in a two dimensional space that covers $\lambda = \eta$. In the extreme case where $\hat{\mathbf{w}} = \mathbf{w}$, we see that $\lambda^* = \eta^*$ if and only if $\rho \frac{\alpha_t}{\alpha_s} = 1$. Since $\alpha_t^2 = \mathbb{E}\|\boldsymbol{\beta}^2\|_2^2$ and $\alpha_s^2 = \mathbb{E}\|\mathbf{w}^2\|_2^2$, they can be viewed as the vector lengths of $\boldsymbol{\beta}$ and \mathbf{w} , respectively. Intuitively, one would think that distTL requires the lengths of two vectors to be roughly the same, or $\alpha_t = \alpha_s$, to achieve the good performance. However, the optimal choices of λ and η demonstrates that this is not the case. Since ρ^2 is the cosine of the angle between the two vectors, it implies that distTL is optimal if and only if the difference vector $\boldsymbol{\beta} - \mathbf{w}$ is orthogonal to \mathbf{w} , as shown in Figure 2. This is a rather strong assumption and it is hard to achieve or interpret in real applications. In contrast, the proposed angleTL depends only on the angle between the source and target parameters, where source and target are treated equally. This explains the flexibility and the potential advantage of our angle-based method.

4 Incorporating multiple source models

In this section, we consider the setting where multiple source models are available, denoted as $\{\hat{\mathbf{w}}_k\}_{k=1, \dots, K}$, and we want to incorporate these source models when fitting a model using the internal target data. In the existence of multiple sources, we hope that our estimator obtained from

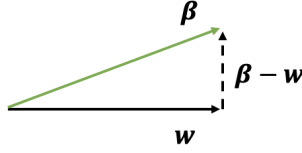


Figure 2: The optimal situation of distance-based transfer learning approach.

transfer learning is robust to the cases where some source models are less helpful than others.

One direct extension of angleTL is to include multiple penalty terms, one for each source estimates $\hat{\mathbf{w}}_k$, and obtain

$$\hat{\beta}_{\lambda, \eta} = \arg \min_{\beta} \frac{1}{n} \|\mathbf{Y} - \mathbf{X}\beta\|_2^2 + \lambda \|\beta\|_2^2 - 2 \sum_{k=1}^K \eta_k \hat{\mathbf{w}}_k^\top \beta,$$

which consists of $K + 1$ tuning parameters, λ and $\{\eta_k\}_{k=1, \dots, K}$. However, this might be computationally less feasible when K is large, since optimization involving a large number of tuning parameters will be challenging both in terms of computational speed and numerical stability. Intuitively, if we can obtain an aggregated model $\hat{\mathbf{w}}$ from $\{\hat{\mathbf{w}}_k\}_{k=1, \dots, K}$, which is closer to the target estimator β , we can directly apply the single source angleTL described in Section 2.

Following this idea, we present in this section two approaches to obtain the aggregated estimator $\hat{\mathbf{w}}$ from the K source estimators $\{\hat{\mathbf{w}}_k\}_{k=1, \dots, K}$, where the main difference between these two approaches lies in whether an independent validation dataset is needed for the aggregation step in addition to the training data. In the existence of an independent validation dataset, we can use it to train a set of weights that linearly combine $\{\hat{\mathbf{w}}_k\}_{k=1, \dots, K}$ to obtain the aggregated estimator $\hat{\mathbf{w}}$. This can be achieved via methods such as the Q-aggregation, summarized in Algorithm 1 below, which is shown to approximate the best linear combination of all models when the validation data is sufficiently large (Rigollet and Tsybakov, 2011; Tsybakov, 2014; Lecué and Rigollet, 2014).

Algorithm 1: Obtain $\hat{\mathbf{w}}$ from a validation dataset

Data: Source estimates $\{\hat{\mathbf{w}}_k\}_{k=1, \dots, K}$ and a validation dataset $\{\hat{\mathbf{X}}, \hat{\mathbf{Y}}\}$

Obtain the weights $\hat{\theta} = (\hat{\theta}_1, \dots, \hat{\theta}_K)^\top$ by: $\hat{\theta} = \arg \min_{\theta} \|\hat{\mathbf{Y}} - \hat{\mathbf{X}}(\sum_{k=1}^K \theta_k \hat{\mathbf{w}}_k)\|_2^2$.

Obtain $\hat{\mathbf{w}} = \sum_{k=1}^K \hat{\theta}_k \hat{\mathbf{w}}_k$.

Result: $\hat{\mathbf{w}}$

Alternatively, one could consider using the following spectral approach, summarized in Algorithm 2, to obtain an aggregated $\hat{\mathbf{w}}$ without a validation dataset. Specifically, we first normalize each $\hat{\mathbf{w}}_k$ to obtain $\bar{\mathbf{w}}_k = \frac{\hat{\mathbf{w}}_k}{\|\hat{\mathbf{w}}_k\|_2}$, and define $\bar{\mathbf{W}} = [\bar{\mathbf{w}}_1^\top, \bar{\mathbf{w}}_2^\top, \dots, \bar{\mathbf{w}}_K^\top]^\top \in \mathbb{R}^{K \times p}$. Let \mathbf{u}_1 be the first eigenvector of $\bar{\mathbf{W}}\bar{\mathbf{W}}^\top \in \mathbb{R}^{K \times K}$, and define $\hat{\mathbf{s}} = (\hat{s}_1, \dots, \hat{s}_K) = |\mathbf{u}_1|$, the absolute value of \mathbf{u}_1 . We

propose to use $\hat{\mathbf{s}}$ as the weights for aggregating the K normalized source estimates. Then the final adaptive weighted source estimates is defined as $\hat{\mathbf{w}} = \sum_{k=1}^K \hat{s}_k \bar{\mathbf{w}}_k$. Intuitively, this approach can be considered as carrying out a principal component (PC) analysis on the matrix $\bar{\mathbf{W}}$ that combines all the source estimators, where \mathbf{u}_1 is the first PC loadings of $\bar{\mathbf{W}}$, under which the linear combination $\mathbf{u}_1^\top \bar{\mathbf{W}}$ of $\hat{\mathbf{w}}_k$'s has the largest variance, or summarizes the most information in $\bar{\mathbf{W}}$. In particular, under suitable conditions (see Theorem 2 below) on the overall quality of the source estimators, the first PC loadings are all nonnegative (in this case $\hat{\mathbf{s}} = \mathbf{u}_1$), so that the first PC, $\bar{\mathbf{W}}^\top \hat{\mathbf{s}}$, is exactly the final consensus source estimator $\hat{\mathbf{w}}$. Moreover, whenever $\{\hat{\mathbf{w}}_k\}_{k=1,\dots,K}$ together contain sufficient amount of information about the direction of β , it can also be shown that the components of $\hat{\mathbf{s}}$ reflect the true discrepancy between each $\hat{\mathbf{w}}_k$ and β , and that the final consensus source estimator is asymptotically no worse than the best candidate source estimator (see Theorem 2 below). Similar spectral weighting idea has been considered for combining multiple classifiers without labeled data (Parisi et al., 2014). Such a strategy avoids splitting extra samples from already limited target data for aggregation so that it does not affect the prediction performance.

Algorithm 2: Obtain $\hat{\mathbf{w}}$ without a validation dataset

Data: Source estimates $\{\hat{\mathbf{w}}_k\}_{k=1,\dots,K}$

for $k = 1, \dots, K$ **do**

 | Normalize $\hat{\mathbf{w}}_k$ and obtain $\bar{\mathbf{w}}_k = \frac{\hat{\mathbf{w}}_k}{\|\hat{\mathbf{w}}_k\|_2}$.

end

Define $\bar{\mathbf{W}} = [\bar{\mathbf{w}}_1^\top, \bar{\mathbf{w}}_2^\top, \dots, \bar{\mathbf{w}}_K^\top]^\top$. Let $\hat{\mathbf{s}} = (\hat{s}_1, \dots, \hat{s}_K) = |\mathbf{u}_1|$, where \mathbf{u}_1 is the first eigenvector of $\bar{\mathbf{W}}\bar{\mathbf{W}}^\top$.

Obtain the aggregated source estimates $\hat{\mathbf{w}} = \sum_{k=1}^K \hat{s}_k \bar{\mathbf{w}}_k$.

Result: $\hat{\mathbf{w}}$

The theoretical guarantee for Algorithm 1 has been carefully studied, e.g., in Tsybakov (2014). Here, we provide theoretical justification for Algorithm 2. We start with some definitions. Similarly as in Section 2, for each $k \in [K]$, we consider $\hat{\mathbf{w}}_k = \mathbf{w}_k + \delta_k$, and assume \mathbf{w}_k and δ_k satisfy Assumptions 2 and 3. Moreover, we define $\mathbf{R}_w = (\rho_{ij}^w) \in \mathbb{R}^{K \times K}$, where $\frac{\rho_{ij}^w}{p}$ is the largest eigenvalue of

$$\mathbb{E} \left[\left(\frac{\mathbf{w}_i}{\|\mathbf{w}_i\|_2} - \frac{\beta}{\|\beta\|_2} \right) \left(\frac{\mathbf{w}_j}{\|\mathbf{w}_j\|_2} - \frac{\beta}{\|\beta\|_2} \right)^\top \right], \quad 1 \leq i, j \leq K, \quad (8)$$

which characterizes the pairwise correlation between the discrepancies in $\frac{\mathbf{w}_i}{\|\mathbf{w}_i\|_2}$ and $\frac{\mathbf{w}_j}{\|\mathbf{w}_j\|_2}$ with respect to $\frac{\beta}{\|\beta\|_2}$, and define $\mathbf{R}_\delta = (\rho_{ij}^\delta) \in \mathbb{R}^{K \times K}$ where $\frac{\rho_{ij}^\delta}{p}$ is the largest eigenvalue of

$$\mathbb{E} \left[\frac{\delta_i \delta_j^\top}{\|\mathbf{w}_i\|_2 \|\mathbf{w}_j\|_2} \right], \quad 1 \leq i, j \leq K \quad (9)$$

which characterizes the pairwise correlation between the normalized source estimation errors $\frac{\delta_i}{\|\mathbf{w}_i\|_2}$ and $\frac{\delta_j}{\|\mathbf{w}_j\|_2}$. In a special case where the source datasets are mutually independent, we have $\rho_{ij}^\delta = 0$

for $i \neq j$, and \mathbf{R}_δ is a diagonal matrix. Finally, we define the true similarity between $\hat{\mathbf{w}}_i$'s and $\boldsymbol{\beta}$ as $\mathbf{s} = (\cos \angle(\hat{\mathbf{w}}_1, \boldsymbol{\beta}), \dots, \cos \angle(\hat{\mathbf{w}}_K, \boldsymbol{\beta}))^\top$. With the above preparation, we state our main results concerning Algorithm 2.

Theorem 2. *Suppose for each $k \in \{1, \dots, K\}$, \mathbf{w}_k and $\boldsymbol{\delta}_k$ satisfy Assumptions 2 and 3 with ρ being bounded away from 0, and that $\|\boldsymbol{\delta}_k\|_2^2 = \mathbb{E}\|\boldsymbol{\delta}_k\|_2^2 \cdot (1 + o(1))$ with high probability¹. Then, for any small constant $\epsilon > 0$, there exists some sufficiently small constant $C_1(\epsilon) > 0$ such that whenever $\max\{\|\mathbf{R}_\delta\|, \|\mathbf{R}_w\|\}/K \leq C_1(\epsilon)$, the following holds:*

1. *For the spectral weights $\hat{\mathbf{s}}$ and the consensus source estimator $\hat{\mathbf{w}}$ defined in Algorithm 2, it holds that $\cos \angle(\hat{\mathbf{s}}, \mathbf{s}) = \frac{\hat{\mathbf{s}}^\top \mathbf{s}}{\|\hat{\mathbf{s}}\|_2 \|\mathbf{s}\|_2} \geq 1 - \epsilon$ and $\cos \angle(\hat{\mathbf{w}}, \boldsymbol{\beta}) > \rho - \epsilon$ in probability as $n \rightarrow \infty$.*
2. *There exists some constant $C_2(\epsilon) > 0$ such that, whenever $\frac{1}{p} \text{tr}(\boldsymbol{\Sigma}_\delta) \geq C_2(\epsilon) \alpha_s^2$, we have $\cos \angle(\hat{\mathbf{w}}, \boldsymbol{\beta}) > \max_{1 \leq k \leq K} \cos \angle(\hat{\mathbf{w}}_k, \boldsymbol{\beta}) + \epsilon$ in probability as $n \rightarrow \infty$.*

Theorem 2 yields the effectiveness of the spectral weighting approach in three aspects. Firstly, it ensures that the estimated weight vector $\hat{\mathbf{s}}$ will converge to the true similarity measure $\mathbf{s} = (\cos \angle(\hat{\mathbf{w}}_1, \boldsymbol{\beta}), \dots, \cos \angle(\hat{\mathbf{w}}_K, \boldsymbol{\beta}))^\top$ as $n \rightarrow \infty$. As a result, more weights will be given to the source estimators closer to $\boldsymbol{\beta}$ and less weights to those with smaller $\cos \angle(\hat{\mathbf{w}}_k, \boldsymbol{\beta})$. Secondly, it indicates the guaranteed performance of the final consensus source estimator $\hat{\mathbf{w}}$, as long as the original correlation ρ between the source and target regression coefficients is sufficiently strong. Thirdly, and interestingly, part two of Theorem 2 shows that, whenever the source estimators have weak signal-to-noise ratio in the sense that $\frac{\mathbb{E}\|\mathbf{w}_k\|_2^2}{\mathbb{E}\|\boldsymbol{\delta}_k\|_2^2} = \frac{p\alpha_s^2}{\text{tr}(\boldsymbol{\Sigma}_\delta)}$ is small, the consensus estimator has strictly better performance than all the source estimators in the large sample limit, demonstrating the consensus power of the spectral weighted estimator. The validity of the method relies on the additional condition that $\max\{\|\mathbf{R}_\delta\|, \|\mathbf{R}_w\|\}$ is small compared with K , which essentially requires the source estimators to be sufficiently diverse and less correlated in terms of both the respective true coefficients \mathbf{w}_k , and the estimation errors $\boldsymbol{\delta}_k$. In general, such a condition is mild for many real applications. In Section 6, we show the effectiveness and superior performance of such spectral weighting approach in combining multiple source estimators learned from different genetic risk models.

5 Simulation study

5.1 Comparing empirical and theoretical predictive risks

We perform a simulation study to verify the theoretical predictive risks shown in Theorem 1. We first consider the noiseless case where the source estimator $\hat{\mathbf{w}} = \mathbf{w}$. For $j \in \{1, \dots, p\}$, we generate

$$(\mathbf{w}_j, \boldsymbol{\beta}_j)^\top \stackrel{i.i.d.}{\sim} N \left(0, \frac{1}{p} \begin{pmatrix} \alpha_s^2 & \rho \alpha_s \alpha_t \\ \rho \alpha_s \alpha_t & \alpha_t^2 \end{pmatrix} \right). \quad (10)$$

¹An even A_n holds with high probability if there exists some $N > 0$ such that for all $n \geq N$ we have $P(A_n) \geq 1 - n^{-D}$ for some large constant $D > 0$.

We set $n = 50$ and $p = \gamma n$, and generate \mathbf{X} from independent standard normal distributions. With \mathbf{X} , we generate $\mathbf{Y} \sim N(\mathbf{X}\boldsymbol{\beta}, 0.5\mathbf{I}_n)$. We vary the signal strength ratio $\frac{\alpha_t}{\alpha_s}$, as well as the dimension-to-sample ratio $\gamma = \frac{p}{n}$ across different settings.

In the noiseless case, we have a precise prediction risk as shown in Equation (7). For a given λ chosen from a grid, we set $\eta = \rho \frac{\alpha_t}{\alpha_s}$, which is the optimal choice of η , and calculate the theoretical risk. We can also obtain the theoretical risk of distTL by setting $\eta = \lambda$ in Equation (7). For the target-only approach, we obtain the theoretical risk by setting $\eta = 0$ in Equation (7). To obtain the empirical predictive risks, we fit each model on the training data for each λ from the grid, and then obtain the corresponding mean square errors evaluated on an independent testing dataset with $n = 100$.

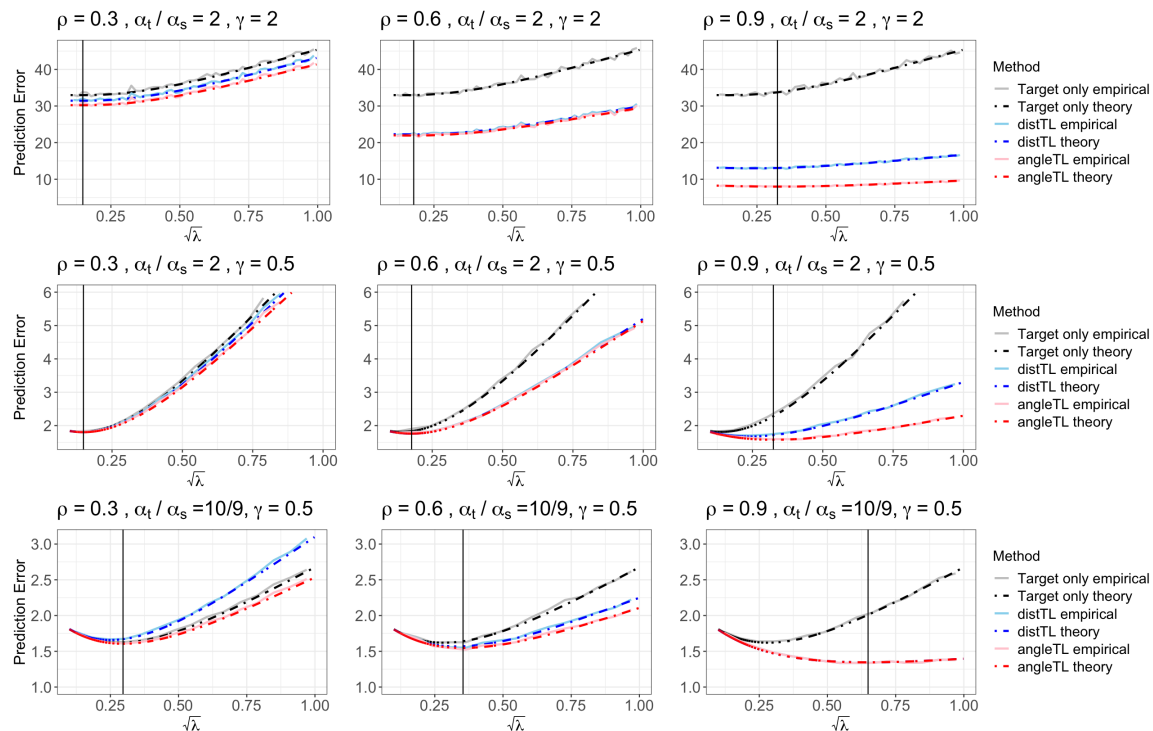


Figure 3: Empirical prediction error over 500 simulation replicates (solid curve) versus theoretical prediction error given in Equation (7) (dashed curve). The vertical line shows the optimal $\sqrt{\lambda}$ in theory that leads to the minimum prediction error. We generate target and source estimates, $\boldsymbol{\beta}$ and \mathbf{w} , through multivariate Gaussian distribution, by varying their correlation $\rho \in \{0.3, 0.6, 0.9\}$ (in columns), signal strength ratio $\frac{\alpha_t}{\alpha_s} \in \{\frac{10}{9}, 2\}$ and dimension-to-sample ratio $\gamma = \frac{p}{n} \in \{2, \frac{1}{2}\}$ (in rows). We sequentially select 100 λ values, and for each λ we train on 50 samples and test on 100 samples. We report the average test error over 500 simulations. Black: target-only model; blue: distTL; red: angleTL.

Figure 3 compares the empirical risks and theoretical risks under the noiseless case. For all methods, the empirical risk aligns perfectly with the empirical risks, demonstrating the theoretical risk we obtained in Equation (7) is precise. As expected, angleTL is no worse than the target-only estimator and distTL across all settings. Moreover, the optimal λ in theory (vertical line) precisely falls on the lowest point of the curve in all settings. Note that in the bottom right panel, we have $\rho \frac{\alpha_t}{\alpha_s} = 1$ which represents the orthogonal case shown in Figure 2 where distTL reaches the same performance as angleTL. However, distTL can be worse than the target-only approach when $\rho \frac{\alpha_t}{\alpha_s}$ is far from 1, e.g., the first column, indicating that it cannot prevent negative transfer.

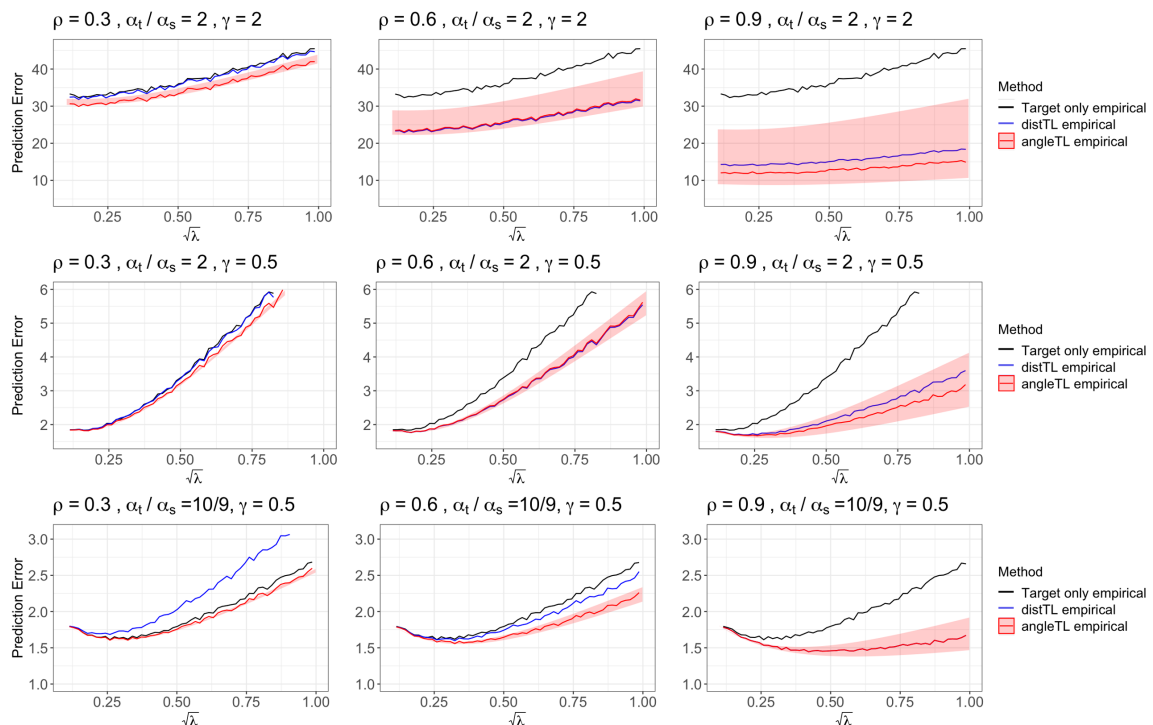


Figure 4: Empirical prediction error over 500 simulation replicates (solid curve) and theoretical prediction error bound of proposed method following Theorem 1 (filled area). We generate target and source estimates, β and \mathbf{w} , through multivariate normal distribution, by varying their correlation $\rho \in \{0.3, 0.6, 0.9\}$ (in columns), signal strength ratio $\frac{\alpha_t}{\alpha_s} \in \{\frac{10}{9}, 2\}$, and dimension-to-sample ratio $\gamma = \frac{p}{n} \in \{2, \frac{1}{2}\}$ (in rows). We add randomly generated and uniformly distributed noise δ to \mathbf{w} . We sequentially take 100 λ values, and for each λ we train on 50 samples and test on 100 samples. We report the average test error over 500 simulations. Black: target-only model; blue: distTL; red: angleTL.

Similarly, we perform a simulation study to verify the predictive risks when there are estimation

errors. We use the same data generating mechanism described above, except that we generate random noises $\boldsymbol{\delta} \sim N(\mathbf{0}, \boldsymbol{\Sigma}_\delta)$, where the covariance matrix $\boldsymbol{\Sigma}_\delta$ is generated by setting an exchangeable correlation to be 0.1 and the variances are uniformly generated between 0 to 0.05. We compute C_L and C_U using $\boldsymbol{\Sigma}_\delta$ and obtain the theoretical upper and lower bounds for the predictive risk. Figure 4 shows the empirical predictive risk of the target-only estimator, distTL, and angleTL. In addition, the shaded area represents the theoretical lower and upper bounds of the predictive risk of angleTL obtained in Theorem 1. We can see that the empirical risk of angleTL falls between the theoretical risk bounds. The width of the risk bounds increases with γ and ρ . Across all scenarios, the upper bounds are lower than the empirical risk of the target-only approach, which shows that angleTL can protect against negative transfer.

5.2 Evaluate the predictive performance across different settings

5.2.1 Single source study

In this section, we evaluate the empirical predictive performance of angleTL in the case with one source study. To mimic the practical situation, we generate data for both the source and target populations based on the corresponding model parameters \mathbf{w} and $\boldsymbol{\beta}$ where the corresponding entries are generated from Equation (10). We set the sample sizes to be $N = 5,000$ for the source population, and $n = 50$ for the target population. The dimension of the model is set to $p \in \{25, 50, 100\}$. For the source population, we generate the predictors $\tilde{\mathbf{X}} \sim N(\mathbf{0}, \tilde{\boldsymbol{\Sigma}})$, where the covariance matrix $\tilde{\boldsymbol{\Sigma}}$ is set to have variances of 1 and exchangeable correlation of 0.2, and we generate the outcome variable $\tilde{\mathbf{Y}} \sim N(\tilde{\mathbf{X}}^\top \mathbf{w}, 0.5\mathbf{I}_N)$. For the target population, we generate $\mathbf{X} \sim N(\mathbf{0}, \boldsymbol{\Sigma})$, where $\boldsymbol{\Sigma}$ contains variances of 1 and exchangeable correlation of 0.1, and we generate the outcome variable $\mathbf{Y} \sim N(\mathbf{X}^\top \boldsymbol{\beta}, 0.5\mathbf{I}_n)$.

For the source data, we apply an ordinary least square approach to obtain $\hat{\mathbf{w}}$, which is then transferred to the target data. We compare the predictive performance of angleTL to three state-of-art methods: (i) target-only: target-only estimator through Equation (1); (ii) source-only: directly apply the source estimates on the testing data; (iii) distTL: distance-based transfer learning approach via Equation (2). The predictive performance is evaluated by the root mean squared error (RMSE) calculated from an independent testing data set of size 200, following the same data generating mechanism as the target data. For each method, the tuning parameters are chosen by a three-fold cross validation.

In Figure 5, each panel of RMSE is summarized from 200 independent simulations, where lower value represents better prediction accuracy. The pattern aligns with what we see in Figures 3, where the performance of angleTL improves over increasing correlation between the target and the source estimates increases. When $\frac{\alpha_t}{\alpha_s} = 2$, we see that distTL overlaps with angleTL around $\rho = \frac{1}{2}$ where $\rho \frac{\alpha_t}{\alpha_s}$ is close to 1. When $\frac{\alpha_t}{\alpha_s} = \frac{1}{2}$, for all $\rho \in (0, 1)$, since $\rho \frac{\alpha_t}{\alpha_s} < \frac{1}{2}$, distTL shows consistently higher RMSE than angleTL; it also underperforms the target-only estimator, indicating that distTL fails

to capture the similarity between the target and the source estimates and fails to prevent negative transfer. For a given $\gamma = \frac{p}{n}$, the performance of angleTL is stable across different values of $\frac{\alpha_t}{\alpha_s}$. For a given $\frac{\alpha_t}{\alpha_s}$, the source model helpful when the dimension of the model is higher.

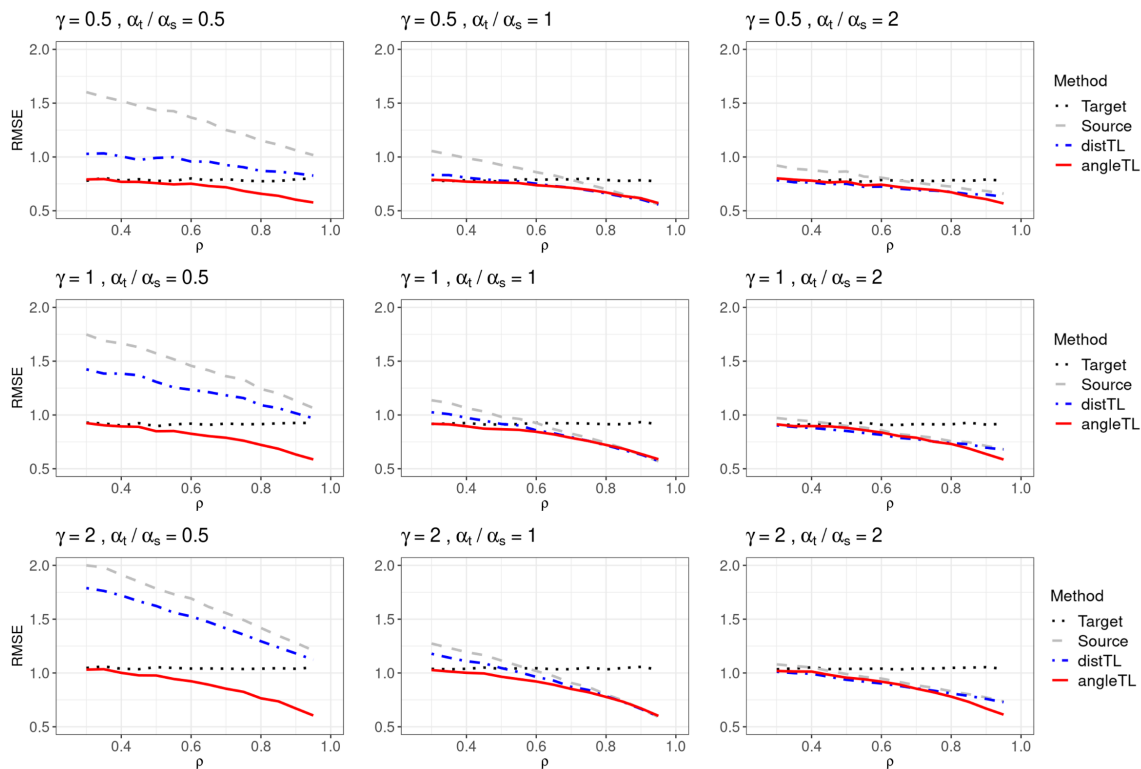


Figure 5: Root mean squared error (RMSE) of predicted outcome over 200 simulations. In each panel, we vary the correlation ρ between the target and source estimates from 0.3 to 0.95. We vary $\gamma = \frac{p}{n} \in \{\frac{1}{2}, 1, 2\}$ (in rows) and the signal strength ratio $\frac{\alpha_t}{\alpha_s} \in \{\frac{1}{2}, 1, 2\}$ (in columns). Black: target-only model; grey: source-only model; blue: distTL; red: angleTL.

5.2.2 Multiple source studies

We also consider the situation where we have multiple source studies as introduced in Section 4. The target sample size is set to $n = 100$ and each source population is of size $N = 5,000$. The two panels of violin plot in Figure 6 represent two configurations, the left shows the case where all source estimates have similar correlation as the target estimates between 0.4 to 0.6 and the right shows the case where some of the sources are much more helpful than others, with correlations ranging from 0.1 to 0.9. In the former case, the proposed angleTL-multi2 that aggregates all source estimates to find a composite direction outperforms angleTL applying on the best single source estimates ($\hat{\mathbf{w}}_5$

with $\rho_5 = 0.6$) and angleTL-multi1 that learns the best linear combination of all source estimates. The later case shows similar pattern, where angleTL applying on the best single source (\hat{w}_5 with $\rho_5 = 0.9$) and angleTL-multi1 show improved performance, slightly worse than angleTL-multi2.

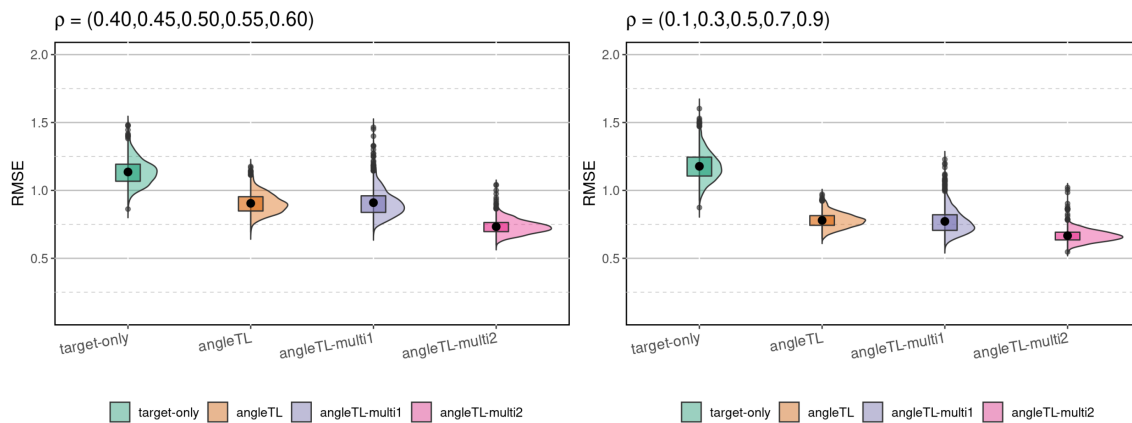


Figure 6: Root mean squared error (RMSE) of predicted outcome over 1,000 simulations for target only estimates (target-only), proposed method for transferring the best single source estimates (angleTL), and proposed methods transferring multi-source estimates (angleTL-multi1 learns the best linear combination of all source estimates and angleTL-multi2 finds a composite direction of all source estimates). The two plots correspond to two configurations with correlation $\rho = (\rho_1, \rho_2, \rho_3, \rho_4, \rho_5)$ being $(0.4, 0.45, 0.5, 0.55, 0.6)$ and $(0.1, 0.3, 0.5, 0.7, 0.9)$, respectively.

6 Application to predict low-density lipoprotein

We apply angleTL, angleTL-multi1, and angleTL-multi2 to predict low-density lipoprotein (LDL) cholesterol, a blood biomarker that plays a crucial role in determining cardiovascular disease (Kwiterovich Jr, 2000), in self-reported White population using data from Mass General Brigham Biobank (MGBB) (Karlson et al., 2016). MGBB is a research database launched in 2021, containing around eighty thousands DNA samples before data quality control, yet still a relatively limited data size compared to other population-based biobanks such as the United Kingdom Biobank (UKB) (Sudlow et al., 2015). In this application, our goal is to build a prediction model for LDL using basic demographic and clinical risk factors, combined with top single nucleotide polymorphisms (SNPs), where our target population is the White population at MGBB. We consider a total of eight source models, including three models trained at UKB (LDL, Apolipoprotein B-100 [ApoB], and triglycerides) and five models for LDL trained at the five participating sites at the electronic Medical Records and GENomics (eMERGE) Network (Gottesman et al., 2013).

In the MGBB database, we extract age, gender, and antihypertensives medications use (a med-

ication that affects lipids level (Kasiske et al., 1995)), as well as the average of the latest five LDL measures for a total of 5,600 self-reported White participants. A total of 5,306 SNPs are included in the model, selected according to linkage disequilibrium and p-values of a genome-wide associate study (GWAS) using all samples from MGBB data, adjusting for age, gender, and the first 20 principle components (PC). We use UKB as one source dataset, from which we identify 409,031 participants with at least one measure of triglycerides, 408,602 participants with at least one measure of LDL, and 407,366 samples with at least one measure of Apo-B, whose self-reported ancestry information and PC-based ancestry prediction by a published algorithm (Zhang et al., 2020) agree to be European. We also include five biobanks from eMERGE, each as a source dataset, and we identify a total of 16,723 samples with at least one LDL measure. We extract the same set of genetic, clinical and demographic variables from UKB and eMERGE, and fit eight source models using ridge regression. A summary of sample sizes, outcome variable, and biobanks can be found in Table 1.

Table 1: Basic information of the target and eight source datasets.

	Biobank	Outcome	Sample size	Mean age (SD)	Male (%)	
Target	MGBB	LDL	5,600	64.7 (15.3)	2,959 (52.8)	
Source	UKB	LDL	408,602	69.8 (8.0)	187,607 (45.9)	
		Tri	409,031	69.8 (8.0)	187,821 (45.9)	
		Apo-B	407,366	69.8 (8.0)	186,763 (45.8)	
	eMERGE	Marshfield Clinic (Marsh)	LDL	4,551	70.8 (9.7)	1,496 (39.2)
		University of Washington (UW)	LDL	618	80.9 (0.5)	295 (54.0)
		Mayo Clinic (Mayo)	LDL	3,185	71.3 (10.1)	1,512 (56.7)
		Northwestern University (NWU)	LDL	3,037	53.4 (15.2)	287 (20.0)
		Mount Sinai Hospital (MtSinai)	LDL	5,332	60.4 (13.1)	363 (69.1)

We compare the performance of the target-only estimator, the source-only estimator, distTL, and angleTL, treating the MGBB data as the target. We randomly split the MGBB data into training and testing with a ratio of 10:1. For angleTL-multi1, which needs validation data for aggregation, we further split 5% from the training data. All methods are trained on the training data, and the performance is measured by the R^2 (variance explained by the model) evaluated on the testing data. This process is repeated 100 times to account for the sampling variability.

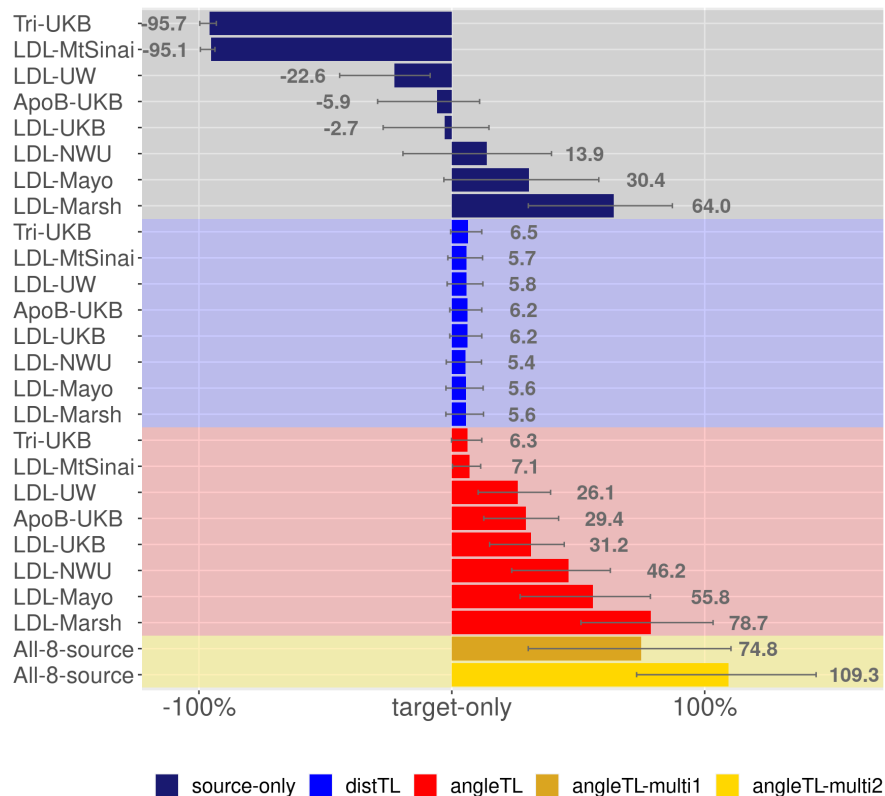


Figure 7: Mean (1st-3rd quantile) percentage change of R^2 compared to the target-only model. The dark blue bars with grey background contains source-only estimates from UKB and eMERGE; the light blue bars with light blue background contains distTL; the red bars with red background includes the proposed single-source angleTL; and the last two yellow rows show angleTL-multi1 and angleTL-multi2, respectively. Tri-UKB: triglycerides from UKB; ApoB: Apolipoprotein B-100; LDL: low-density lipoprotein; MtSinai=Mount Sinai Hospital, UW=University of Washington, NWU=Northwestern University, Mayo=Mayo Clinic, and Marsh=Marshfield Clinic.

In Figure 7, we present the relative performance of each method compared to the benchmark target-only model. With 100 replications, we report the mean, the first and the third quantiles of the percentage improvement of R^2 . Among all the source-only models (dark blue bars with grey background), the model trained at UKB using triglycerides as the outcome has the worse performance, and the model trained at Marshfield Clinic has the highest performance, where the average improvement is around 64%. When transferring each source model to train the target model using distTL (light blue bars with light blue background), all the single-source distTL have similar performance, around 6% improvement. When applying single-source angleTL (red bars with red background), we observe that the performance is uniformly better than the corresponding source-

only models, and angleTL also outperforms distTL. In the last two rows, we see that angleTL-multi1 has comparable performance as the best single source, LDL-Marsh, while angleTL-multi2 has the largest improvement of 109.3%.

7 Discussion

We propose angleTL, a flexible transfer learning framework that leverages the concordance of model parameters across populations. Compared to benchmark methods, including the target-only model, the source-only models, and the existing transfer learning methods based on penalizing the distance between two sets of model parameters, angleTL is shown to have improved performance both empirically and numerically. Under the setting with a single source model, we identify factors that affect angleTL’s performance, including (1) the similarity between model parameters measured by the $\sin \Theta$ distance, (2) the signal strengths of the source and the target model, (3) the ratio between model dimensionality and the target sample size, (4) the estimation error of the source model, and (5) the level of the noise, which provide useful practical guidance for understanding when a source population can be helpful. With multiple source models, we propose to aggregate the source models first before applying angleTL, which we also provide theoretical justifications of the aggregation algorithms. Like ridge regression, angleTL is easy-to-implement as it enjoys the advantage of having a closed-form solution. It does not require individual-level data from the source, and can prevent negative transfer. Our simulation and real data application demonstrate the validity and feasibility of angleTL across a wide range of settings.

One limitation of angleTL is that it requires the source and the target models to include the same covariates, whereas, in practice, source models might include covariates that are not measured at the target data or vice versa. There are existing methods focusing on incorporating source models that use a subset of covariates in the target model. For example, Chatterjee et al. (2016) proposed a constrained maximized likelihood approach where the external data follows the same distribution as the internal data. Accounting for heterogeneous data, methods such as Estes et al. (2018); Kundu et al. (2019); Zhang et al. (2020); Gu et al. (2020); Taylor et al. (2022) are proposed, which all considered low-dimensional models and their ability to handle high-dimensional data requires further investigation. A more detailed discussion on related work, including different empirical approaches, can be found in Han (2022). It is an interesting future direction to extend angleTL to the setting where the source study uses a subset of the covariates in the target study. Methods proposed in related work such as Taylor et al. (2022) can be considered to address this, where we can first map the unique variables to a space orthogonal to the shared variables, and then include them in the model while using the angle-based regularization to borrow information.

Although we use a linear model to illustrate angleTL, the penalty term $\lambda \|\beta\|_2^2 - 2\eta \hat{\mathbf{w}}^\top \beta$ can be combined with objective functions of other models such as the generalized linear models (Nelder and Wedderburn, 1972), the Cox model (Therneau and Grambsch, 2000), support vector machine

(Cortes and Vapnik, 1995), and linear or quadratic discrimination analysis (Hastie et al., 2009). Similarly, while the angle-based similarity measure introduced in our work is based on the L_2 norm, corresponding to the angle defined in the Euclidean space, it may be extended to other non-Euclidean spaces, which is worth further investigation.

References

- Belbasis, L. and O. A. Panagiotou (2022). Reproducibility of prediction models in health services research. *BMC Research Notes* 15(1), 1–5.
- Cai, T., M. Liu, and Y. Xia (2021). Individual data protected integrative regression analysis of high-dimensional heterogeneous data. *Journal of the American Statistical Association*, 1–15.
- Cai, T. T., X. Han, and G. Pan (2020). Limiting laws for divergent spiked eigenvalues and largest nonspiked eigenvalue of sample covariance matrices. *The Annals of Statistics* 48(3), 1255–1280.
- Chatterjee, N., Y.-H. Chen, P. Maas, and R. J. Carroll (2016). Constrained maximum likelihood estimation for model calibration using summary-level information from external big data sources. *Journal of the American Statistical Association* 111, 107–117.
- Chen, E. Y., M. I. Jordan, and S. Li (2022). Transferred q-learning. *arXiv preprint arXiv:2202.04709*.
- Chen, W.-C., C. Wang, H. Li, N. Lu, R. Tiwari, Y. Xu, and L. Q. Yue (2020). Propensity score-integrated composite likelihood approach for augmenting the control arm of a randomized controlled trial by incorporating real-world data. *Journal of Biopharmaceutical Statistics* 30(3), 508–520.
- Cortes, C. and V. Vapnik (1995). Support-vector networks. *Machine learning* 20(3), 273–297.
- Dobriban, E. and S. Wager (2018). High-dimensional asymptotics of prediction: Ridge regression and classification. *The Annals of Statistics* 46(1), 247–279.
- Donoho, D. and M. Gavish (2014). Minimax risk of matrix denoising by singular value thresholding. *The Annals of Statistics* 42(6), 2413–2440.
- Duan, R., M. R. Boland, J. H. Moore, and Y. Chen (2018). Odal: A one-shot distributed algorithm to perform logistic regressions on electronic health records data from multiple clinical sites. In *BIOCOMPUTING 2019: Proceedings of the Pacific Symposium*, pp. 30–41. World Scientific. PMID: PMC6417819.
- Duan, R., C. Luo, M. J. Schuemie, J. Tong, C. J. Liang, H. H. Chang, M. Regina Boland, J. Bian, H. Xu, J. H. Holmes, C. B. Forrest, S. C. Morton, J. A. Berlin, J. H. Moore, K. B. Mahoney, and

- Y. Chen (2020). Learning from local to global: An efficient distributed algorithm for modeling time-to-event data. *Journal of the American Medical Informatics Association* 27(7), 1028–1036.
- Duan, R., Y. Ning, and Y. Chen (2022). Heterogeneity-aware and communication-efficient distributed statistical inference. *Biometrika* 109(1), 67–83.
- Duan, Y. and K. Wang (2022). Adaptive and robust multi-task learning. *arXiv preprint arXiv:2202.05250*.
- Estes, J. P., B. Mukherjee, and J. M. Taylor (2018). Empirical bayes estimation and prediction using summary-level information from external big data sources adjusting for violations of transportability. *Statistics in biosciences* 10(3), 568–586.
- Ganin, Y. and V. Lempitsky (2015). Unsupervised domain adaptation by backpropagation. In *International conference on machine learning*, pp. 1180–1189. PMLR.
- Girshick, R., J. Donahue, T. Darrell, and J. Malik (2014). Rich feature hierarchies for accurate object detection and semantic segmentation. In *Proceedings of the IEEE conference on computer vision and pattern recognition*, pp. 580–587.
- Gottesman, O., H. Kuivaniemi, G. Tromp, W. A. Faucett, R. Li, T. A. Manolio, S. C. Sanderson, J. Kannry, R. Zinberg, M. A. Basford, et al. (2013). The electronic medical records and genomics (eMERGE) network: past, present, and future. *Genetics in Medicine* 15(10), 761–771. PMID: PMC3795928.
- Gu, T., Y. Han, and R. Duan (2023). A transfer learning approach based on random forest with application to breast cancer prediction in underrepresented populations. In *proceedings in Pacific Symposium on Biocomputing (PSB)*.
- Gu, T., P. H. Lee, and R. Duan (2022). Commute: communication-efficient transfer learning for multi-site risk prediction. *MedRxiv*.
- Gu, T., J. M. Taylor, and B. Mukherjee (2020). A meta-inference framework to integrate multiple external models into a current study. *arXiv preprint arXiv:2010.09971*.
- Hafemeister, C. and R. Satija (2019). Normalization and variance stabilization of single-cell rna-seq data using regularized negative binomial regression. *Genome biology* 20(1), 1–15.
- Han, P. (2022). A discussion on “a selective review of statistical methods using calibration information from similar studies” by qin, liu and li. *Stat. Theory Relat. Fields*, 1–3.
- Hastie, T., R. Tibshirani, J. H. Friedman, and J. H. Friedman (2009). *The elements of statistical learning: data mining, inference, and prediction*, Volume 2. Springer.

- Hoerl, A. E. and R. Kennard (1970). Ridge regression: biased estimation for nonorthogonal problems. *Technometrics* 12.
- Huang, J., A. Gretton, K. Borgwardt, B. Schölkopf, and A. Smola (2006). Correcting sample selection bias by unlabeled data. *Advances in neural information processing systems* 19.
- Jia, J. and T. Shi (2017). Towards efficiency in rare disease research: what is distinctive and important? *Science China Life Sciences* 60(7), 686–691.
- Karlson, E. W., N. T. Boutin, A. G. Hoffnagle, and N. L. Allen (2016). Building the partners healthcare biobank at partners personalized medicine: Informed consent, return of research results, recruitment lessons and operational considerations. *Journal of Personalized Medicine* 6(1). PMID: PMC4810381.
- Kasiske, B. L., J. Z. Ma, R. S. Kalil, and T. A. Louis (1995). Effects of antihypertensive therapy on serum lipids. *Annals of internal medicine* 122(2), 133–141.
- Kim, P. and E. L. Milliken (2019). Minority participation in biobanks: An essential key to progress. *Biobanking*, 43–50.
- Kirby, J. C., P. Speltz, et al. (2016). Phekb: a catalog and workflow for creating electronic phenotype algorithms for transportability. *JAMIA* 23(6), 1046–1052.
- Kundu, P., R. Tang, and N. Chatterjee (2019). Generalized meta-analysis for multiple regression models across studies with disparate covariate information. *Biometrika* 106(3), 567–585.
- Kwiterovich Jr, P. O. (2000). The metabolic pathways of high-density lipoprotein, low-density lipoprotein, and triglycerides: a current review. *The American journal of cardiology* 86(12), 5–10.
- Lecué, G. and P. Rigollet (2014). Optimal learning with q-aggregation. *The Annals of Statistics* 42(1), 211–224.
- Ledoit, O. and M. Wolf (2015). Spectrum estimation: A unified framework for covariance matrix estimation and pca in large dimensions. *Journal of Multivariate Analysis* 139, 360–384.
- Li, C., C. Yang, J. Gelernter, and H. Zhao (2014). Improving genetic risk prediction by leveraging pleiotropy. *Human Genetics* 133(5), 639–650.
- Li, S., T. Cai, and R. Duan (2021). Targeting underrepresented populations in precision medicine: A federated transfer learning approach. *arXiv preprint arXiv:2108.12112*.
- Li, S., T. T. Cai, and H. Li (2020). Transfer learning for high-dimensional linear regression: Prediction, estimation, and minimax optimality. *Journal of the Royal Statistical Society Series B* 84(1).

- Li, S., T. T. Cai, and H. Li (2022). Transfer learning in large-scale gaussian graphical models with false discovery rate control. *Journal of the American Statistical Association*, 1–13.
- Li, X. and Y. Song (2020). Target population statistical inference with data integration across multiple sources—an approach to mitigate information shortage in rare disease clinical trials. *Statistics in Biopharmaceutical Research* 12, 322–333.
- Liang, M., X. Zhong, and J. Park (2020). Learning a high-dimensional classification rule using auxiliary outcomes. *arXiv preprint arXiv:2011.05493*.
- Lin, H. and M. Reimherr (2022). On transfer learning in functional linear regression. *arXiv preprint arXiv:2206.04277*.
- Liu, Y., T. Fan, T. Chen, Q. Xu, and Q. Yang (2021). Fate: An industrial grade platform for collaborative learning with data protection. *J. Mach. Learn. Res.* 22(226), 1–6.
- Long, M., J. Wang, G. Ding, J. Sun, and P. S. Yu (2013). Transfer feature learning with joint distribution adaptation. In *Proceedings of the IEEE international conference on computer vision*, pp. 2200–2207.
- Maier, R., G. Moser, G.-B. Chen, S. Ripke, and Cross-Disorder Working Group of the Psychiatric Genomics Consortium (2014). Joint analysis of psychiatric disorders increases accuracy of risk prediction for schizophrenia, bipolar disorder, and major depressive disorder. *The American Journal of Human Genetics* 96(2), 283–294.
- Mansukhani, M. P., B. P. Kolla, Z. Wang, and T. I. Morgenthaler (2019). Effect of varying definitions of hypopnea on the diagnosis and clinical outcomes of sleep-disordered breathing: a systematic review and meta-analysis. *Journal of Clinical Sleep Medicine* 15(5), 687–696.
- Miglioretti, D. L. (2003). Latent transition regression for mixed outcomes. *Biometrics* 59(3), 710–720.
- Mitchell, B. L., J. G. Thorp, Y. Wu, A. I. Campos, D. R. Nyholt, S. D. Gordon, D. C. Whiteman, C. M. Olsen, I. B. Hickie, N. G. Martin, et al. (2021). Polygenic risk scores derived from varying definitions of depression and risk of depression. *JAMA psychiatry* 78(10), 1152–1160.
- Nelder, J. A. and R. W. Wedderburn (1972). Generalized linear models. *Journal of the Royal Statistical Society: Series A (General)* 135(3), 370–384.
- Pan, S. J., I. W. Tsang, J. T. Kwok, and Q. Yang (2010). Domain adaptation via transfer component analysis. *IEEE transactions on neural networks* 22(2), 199–210.
- Parisi, F., F. Strino, B. Nadler, and Y. Kluger (2014). Ranking and combining multiple predictors without labeled data. *Proceedings of the National Academy of Sciences* 111(4), 1253–1258.

- Rigollet, P. and A. Tsybakov (2011). Exponential screening and optimal rates of sparse estimation. *The Annals of Statistics* 39(2), 731–771.
- Roobol, M. J., H. A. van Vugt, S. Loeb, X. Zhu, M. Bul, C. H. Bangma, A. G. van Leenders, E. W. Steyerberg, and F. H. Schröder (2012). Prediction of prostate cancer risk: the role of prostate volume and digital rectal examination in the erspc risk calculators. *European urology* 61(3), 577–583.
- Stearns, F. W. (2010). One hundred years of pleiotropy: a retrospective. *Genetics* 186(3), 767–773.
- Sudlow, C., J. Gallacher, N. Allen, V. Beral, P. Burton, J. Danesh, P. Downey, P. Elliott, J. Green, M. Landray, B. Liu, P. Matthews, G. Ong, J. Pell, A. Silman, A. Young, T. Sprosen, T. Peakman, and R. Collins (2015, 03). Uk biobank: an open access resource for identifying the causes of a wide range of complex diseases of middle and old age. *PLoS medicine* 12(3), e1001779–e1001779.
- Sun, B. and K. Saenko (2016). Deep coral: Correlation alignment for deep domain adaptation. In *European conference on computer vision*, pp. 443–450. Springer.
- Tan, Z. (2006). Regression and weighting methods for causal inference using instrumental variables. *Journal of the American Statistical Association* 101(476), 1607–1618.
- Taylor, J. M., K. Choi, and P. Han (2022). Data integration: Exploiting ratios of parameter estimates from a reduced external model. *Biometrika*.
- Teja, A. (2017). Indonesian fintech business: New innovations or foster and collaborate in business ecosystems? *The Asian Journal of Technology Management* 10(1), 10.
- Therneau, T. M. and P. M. Grambsch (2000). The cox model. In *Modeling survival data: extending the Cox model*, pp. 39–77. Springer.
- Thompson, I. M., D. P. Ankerst, C. Chi, P. J. Goodman, C. M. Tangen, M. S. Lucia, Z. Feng, H. L. Parnes, and C. A. Coltman Jr (2006). Assessing prostate cancer risk: results from the prostate cancer prevention trial. *Journal of the National Cancer Institute* 98(8), 529–534.
- Tian, Y., H. Weng, and Y. Feng (2022). Unsupervised multi-task and transfer learning on gaussian mixture models. *arXiv preprint arXiv:2209.15224*.
- Tian, Y. and F. Yang (2022). Transfer learning under high-dimensional generalized linear models. *Journal of the American Statistical Association*.
- Tsybakov, A. B. (2014). Aggregation and minimax optimality in high-dimensional estimation. In *Proceedings of the International Congress of Mathematicians*, Volume 3, pp. 225–246.
- Tzeng, E., J. Hoffman, N. Zhang, K. Saenko, and T. Darrell (2014). Deep domain confusion: Maximizing for domain invariance. *arXiv preprint arXiv:1412.3474*.

- Van Buuren, S., J. P. L. Brand, C. G. M. Groothuis-Oudshoorn, and D. B. Rubin (2006). Fully conditional specification in multivariate imputation. *Journal of Statistical Computation and Simulation* 76, 1049–1064.
- Viele, K., S. Berry, B. Neuenschwander, B. Amzal, F. Chen, N. Enas, B. Hobbs, J. G. Ibrahim, N. Kinnersley, S. Lindborg, S. Micallef, S. Roychoudhury, and L. Thompson (2014). Use of historical control data for assessing treatment effects in clinical trials. *Pharmaceutical Statistics* 13, 41–54.
- Weiss, K., T. M. Khoshgoftaar, and D. Wang (2016). A survey of transfer learning. *Journal of Big data* 3(1), 1–40.
- Wu, X., R. C. Nethery, M. B. Sabath, D. Braun, and F. Dominici (2020). Exposure to air pollution and covid-19 mortality in the united states: A nationwide cross-sectional study. *MedRxiv*.
- Wynants, L., B. Van Calster, G. S. Collins, R. D. Riley, G. Heinze, E. Schuit, M. M. Bonten, D. L. Dahly, J. A. Damen, T. P. Debray, et al. (2020). Prediction models for diagnosis and prognosis of covid-19: systematic review and critical appraisal. *bmj* 369.
- Yang, F., S. Liu, E. Dobriban, and D. P. Woodruff (2021). How to reduce dimension with pca and random projections? *IEEE Transactions on Information Theory* 67(12), 8154–8189.
- Yang, S. and J. K. Kim (2020). Statistical data integration in survey sampling: a review. *Japanese Journal of Statistics and Data Science* 3, 625–650.
- Zhang, D., R. Dey, and S. Lee (2020). Fast and robust ancestry prediction using principal component analysis. *Bioinformatics* 36(11).
- Zhang, H., L. Deng, M. Schiffman, J. Qin, and K. Yu (2020). Generalized integration model for improved statistical inference by leveraging external summary data. *Biometrika* 107(3), 689–703.